Postprint of: Kozieł S., Bekasiewicz A., Implicit Space Mapping for Variable-Fidelity EM-Driven Design of Compact Circuits, IEEE Antennas and Wireless Propagation Letters, Vol. 28, iss. 4 (2018), pp. 275-277, DOI: 10.1109/LMWC.2018.2811253

Implicit Space Mapping for Variable-Fidelity EM-Driven Design of Compact Circuits

S. Koziel, *Senior Member, IEEE* and A. Bekasiewicz, *Member, IEEE*

***Abstract*—Space mapping (SM) belongs to the most successful surrogate-based optimization (SBO) methods in microwave engineering. Among available SM variations, implicit SM (ISM) is particularly attractive due to its simplicity and separation of extractable surrogate model parameters and design variables of the circuit/system at hand. Unlike other SM approaches, ISM exploits a set of preassigned parameters to align the surrogate with the high-fidelity EM model. However, application of ISM is challenging if equivalent network model of the structure is unavailable or of poor quality. In this letter, a modified ISM that exploits variable-fidelity EM simulation models is proposed. Here, preassigned parameters are introduced in the coarsely-discretized EM surrogate by dividing the substrate below selected components of the structure into segments with different permittivity and common thickness. The proposed method has been verified (also experimentally) using a rat-race coupler and favorably compared with state-of-the-art SBO methods.**

***Index Terms*—EM-driven design, compact couplers, surrogate modeling, implicit space mapping, substrate segmentation.**

I. Introduction

CONTEMPORARY microwave structures are often characterized by complex and densely arranged geometries with considerable electromagnetic (EM) cross-couplings [1]. Therefore, full-wave EM simulations are the only tools for reliable evaluation of their performance. Due to high evaluation cost of EM models, utilization of conventional algorithms for optimization of modern structures is computationally challenging [1], although some of recent developments make them more suitable for RF design [2].

This problem can be mitigated using adjoint sensitivity techniques, where cheap derivative information speeds up gradient optimization [4]. Surrogate-based optimization (SBO) is another class of methods that can be utilized to reduce the design cost of microwave circuits [5]. The key idea behind SBO is to shift the optimization burden to the fast surrogate model which is iteratively corrected using high-fidelity simulation data [6]. The SBO concept is the basis for methods such as space mapping (SM), manifold mapping, and various response correction techniques [5]. Arguably, SM belongs to the most popular SBO techniques in microwave engineering.

Manuscript submitted on December 4, 2017, accepted on February 21, 2018. This work is partially supported by the Icelandic Centre for Research (RANNIS) Grant 174114051, and by National Science Centre of Poland Grant 2015/17/B/ST6/01857.

S. Koziel and A. Bekasiewicz are with the School of Science and Engineering, Reykjavik University, Reykjavik, Iceland (e-mail: koziel@ru.is, bekasiewicz@ru.is), and with the Faculty of Electronics, Telecommunications and Informatics, Gdansk University of Technology, Gdansk, Poland.

Implicit space mapping (ISM) is a variation of SM that exploits so-called preassigned parameters to align the low-fidelity model with the high-fidelity one [7]. Typical ISM parameters for microwave circuits are height and permittivity set for the selected structure segments [5]. ISM is well suited for constrained optimization problems because adjustment of preassigned parameters do not alter the domain of the low-fidelity model. Moreover, the method is simple to implement. Nonetheless, its applicability is limited to geometrically simple structures with reliable equivalent circuit models.

In this letter, generalization of ISM to design of complex circuits represented using coarsely-discretized EM surrogates is proposed. The method exploits variable-fidelity EM models with substrate divided into segments of different permittivity, yet with the same thickness (necessary to ensure consistency of the computational model). Our considerations are illustrated using a compact rat-race coupler. We investigate the effect of the number of preassigned parameters on EM-based ISM performance. The method is compared against state-of-the-art SBO algorithms. Experimental results are also provided.

II. EM-Based Implicit Space Mapping

In this section, we briefly recall the SM methodology [5]. Then, we explain the concept of dividing the substrate into segments and describe implementation of the proposed variable-fidelity EM-based ISM. Numerical results and experimental validation are provided in Section III.

A. Space Mapping

Let $\boldsymbol{R}_f(\boldsymbol{x})$ be a response of the high-fidelity EM model at the design $\boldsymbol{x}$ and U be an objective function. The design optimization problem can be formulated as [7]

$$\boldsymbol{x}^* = \arg\min_{\boldsymbol{x}} U(\boldsymbol{R}_f(\boldsymbol{x})) \tag{1}$$

SM generates a series $\boldsymbol{x}^{(i)}$, i = 0, 1, …, of approximations to the optimal design $\boldsymbol{x}^*$ by solving

$$\boldsymbol{x}^{(i+1)} = \arg\min_{\boldsymbol{x}} U(\boldsymbol{R}_s^{(i)}(\boldsymbol{x})) \tag{2}$$

Here, $\boldsymbol{R}_s^{(i)}$ is an ith surrogate constructed by correction of the coarse model $\boldsymbol{R}_c$. For SM, the $\boldsymbol{R}_s^{(i)}$ model can be rewritten as

$$\boldsymbol{R}_s^{(i)}(\boldsymbol{x}) = \boldsymbol{R}_s^{\#}(\boldsymbol{x}, \boldsymbol{p}^{(i)}) \tag{3}$$

with $\boldsymbol{R}_s^{\#}$ being a generic SM surrogate with parameters $\boldsymbol{p}^{(i)}$ obtained through the parameter extraction (PE) process

$$\boldsymbol{p}^{(i)} = \arg\min_{\boldsymbol{p}} \| \boldsymbol{R}_f(\boldsymbol{x}^{(i)}) - \boldsymbol{R}_s^{\#}(\boldsymbol{x}^{(i)}, \boldsymbol{p}) \| \tag{4}$$

Note that PE in (4) is performed only for the latest design $\boldsymbol{x}^{(i)}$ but multi-point extraction is also possible [7].

B. Substrate Segmentation for EM-based ISM

ISM is a space mapping variant where the parameters $\boldsymbol{p}$ utilized in PE are not, in general, associated with design variables $\boldsymbol{x}$ [5]. Instead, ISM introduces a separate set of degrees of freedom which are adjustable in the surrogate, yet fixed for the fine model. For planar structures, these are normally the substrate parameters (height h and permittivity ε) of the selected segments identified in the equivalent circuit model of the structure at hand [5], [7].

In this work, we propose ISM implemented at the level of coarsely-discretized EM model where preassigned parameters $\boldsymbol{p}$ are implemented by dividing substrate into segments with varying permittivity (cf. Fig. 1) and with common (yet adjustable) thicknesses. Clearly, arrangement of the segments is performed based on engineering experience. Investigations related to their composition will be considered elsewhere.

C. EM-Based Implicit SM

The EM-based ISM proposed here is combined with frequency SM (FSM) and output SM (OSM) because both approaches have no effect on computational cost of the PE process [5], [7]. The surrogate model is defined as

$$\boldsymbol{R}_s^{(i)}(\boldsymbol{x}) = \boldsymbol{R}_c(\boldsymbol{x}, \boldsymbol{p}^{(i)}, F^{(i)}(\Omega)) + \boldsymbol{d}^{(i)} \tag{5}$$

where $\boldsymbol{p} = [\varepsilon_1 \ \ldots \ \varepsilon_N \ h]^T$ with N being the number of segments (cf. Fig 1). Note that $\boldsymbol{R}_c$ explicitly depends on preassigned parameters $\boldsymbol{p}$ and the frequency sweep $\Omega = [\omega_1 \ \ldots \ \omega_m]$. Here, we use notation $\boldsymbol{R}_c(\boldsymbol{x},\boldsymbol{p},\Omega) = [R_c(\boldsymbol{x},\boldsymbol{p},\omega_1) \ \ldots \ R_c(\boldsymbol{x},\boldsymbol{p},\omega_m)]^T$.

Evaluation cost of the coarse-mesh EM model $\boldsymbol{R}_c$ is high compared to that of the equivalent circuit model. Thus, the number of $\boldsymbol{R}_c$ evaluations during PE (4) and surrogate optimization (SO) must be low. In order to ensure this, the ISM parameters $\boldsymbol{p}^{(i)}$ are extracted iteratively as follows

$$\boldsymbol{p}^{(i.k+1)} = \arg\min_{\|\boldsymbol{p}-\boldsymbol{p}^{(i.k)}\| \le \delta_p^{(k)}} \| \boldsymbol{R}_f(\boldsymbol{x}^{(i)}) - \boldsymbol{L}_p^{(k)}(\boldsymbol{x}^{(i)}, \boldsymbol{p}, \Omega) \| \tag{6}$$

where

$$\boldsymbol{L}_p^{(k)} = \boldsymbol{R}_c(\boldsymbol{x}^{(i)},\boldsymbol{p}^{(i.k)},\Omega) + \boldsymbol{J}_p(\boldsymbol{x}^{(i)},\boldsymbol{p}^{(i-1)},\Omega)\cdot(\boldsymbol{p} - \boldsymbol{p}^{(i.k)}) \tag{7}$$

Here, $\boldsymbol{p}^{(i.k)}$, $k = 0, 1, \ldots$, is an approximation of $\boldsymbol{p}^{(i)}$ (note that $\boldsymbol{p}^{(i.0)} = \boldsymbol{p}^{(i-1)}$) and $\boldsymbol{J}_p(\boldsymbol{x}^{(i)},\boldsymbol{p}^{(i-1)},\Omega)$ is an approximation of the Jacobian of $\boldsymbol{R}_c$ with respect to $\boldsymbol{p}$ obtained through finite differentiation (FD). The PE process (6) is embedded in a trust region (TR) framework [8]. The TR radius $\delta_p^{(k)}$ is updated using standard rules [8]. Low cost of PE (only a few simulations of $\boldsymbol{R}_c$) is ensured by keeping $\boldsymbol{J}_p$ unchanged throughout the iterations of (6).

The FSM is implemented by using a polynomial scaling of the following form $F^{(i)}(\omega) = f_{0.i} + f_{0.i}\omega + f_{0.i}\omega^2$ with f_k obtained through minimization of $\|\boldsymbol{R}_f(\boldsymbol{x}^{(i)} - \boldsymbol{R}_c(\boldsymbol{x}^{(i)},\boldsymbol{p}^{(i)},F^{(i)}(\Omega))\|$. The cost of the process is negligible because the frequency scaled $\boldsymbol{R}_c$ is interpolated (from Ω to $F^{(i)}(\Omega)$).

The term $\boldsymbol{d}^{(i)}$ is obtained as $\boldsymbol{d}^{(i)} = \boldsymbol{R}_f(\boldsymbol{x}^{(i)} - \boldsymbol{R}_c(\boldsymbol{x}^{(i)},\boldsymbol{p}^{(i)},F^{(i)}(\Omega))$. It ensures $\boldsymbol{R}_s^{(i)}(\boldsymbol{x}^{(i)}) = \boldsymbol{R}_f(\boldsymbol{x}^{(i)})$ at the beginning of each iteration.

The SO is performed by generating a series $\boldsymbol{x}^{(i+1.k)}$, $k = 0, 1, \ldots$, of approximations to $\boldsymbol{x}^{(i+1)}$ (here, $\boldsymbol{x}^{(i+1.0)} = \boldsymbol{x}^{(i)}$) as

$$\boldsymbol{x}^{(i+1.k+1)} = \arg\min_{\|\boldsymbol{x}-\boldsymbol{x}^{(i+1.k)}\| \le \delta_{SO}^{(k)}} U(\boldsymbol{G}_s^{(i.k)}(\boldsymbol{x})) \tag{8}$$

with $\boldsymbol{G}_s^{(i.k)}(\boldsymbol{x}) = \boldsymbol{R}_s^{(i)}(\boldsymbol{x}^{(i+1.k)} + \boldsymbol{J}_{\boldsymbol{R}c}(\boldsymbol{x}^{(i+1.k)},\boldsymbol{p}^{(i)},F^{(i)}(\Omega))\cdot(\boldsymbol{x} - \boldsymbol{x}^{(i+1.k)})$. Similarly as in (6), $\boldsymbol{J}_{\boldsymbol{R}c}$ (obtained w.r.t. $\boldsymbol{x}$ using FD) is not updated during iterations of (2) to maintain a low cost of SO.

III. Case Study

Our design example is a 3-dB rat-race coupler (RRC) shown in Fig. 2(a) [1]. The structure is implemented on a 0.762 mm thick Taconic RF-35 substrate (ε_r = 3.5, tanδ = 0.0018). The design variables are $\boldsymbol{x} = [w_1 \ \ l_1 \ \ w_2 \ \ l_2 \ \ w_3]^T$. The relative parameters $l_3 = 19w_1 + 18w_2 + w_3 - l_1$, $l_4 = 5w_1 + 6w_2 + l_2 + w_3$, $l_5 = 3w_1 + 4w_2$, and $w_4 = 9w_1 + 8w_2$ ensure consistency of the design (all in mm). Dimension w_0 = 1.7 mm. Design objectives are: (i) $||S_{21}| - |S_{31}|| \le 0.1$ dB at 1 GHz frequency, as well as (ii) $|S_{11}| \le -20$ dB and $|S_{41}| \le -20$ dB in 875 MHz to 1.135 GHz band. The starting point for the optimization is $\boldsymbol{x}^{(0)} = [0.35 \ 4.0 \ 0.35 \ 2.0 \ 0.35]^T$ (chosen arbitrarily for the purpose of demonstrating performance of the proposed algorithm; see Fig. 2(b)).

The structure is implemented in CST Studio. Note, that 3D solver is required to divide substrate into segments with different permittivity. The high-fidelity model $\boldsymbol{R}_f$ consists of ~330,000 cells and its average simulation time on a dual Intel Xeon E5540 machine is 24 min. The low-fidelity model $\boldsymbol{R}_c$ has ~42,000 cells and its simulation time is 120 s. The $\boldsymbol{R}_c$ model is configured so that substrate permittivity below the selected RRC segments can be set individually (cf. Fig. 1).

We consider different substrate partitioning schemes with three ($\boldsymbol{R}_{c1}$), five ($\boldsymbol{R}_{c2}$), and seven ($\boldsymbol{R}_{c3}$) segments (cf. Fig. 1). A comparison of the high-fidelity model responses at the selected design with the responses of adjusted ISM surrogates (enhanced by FSM) is shown in Fig. 3. The results indicate that the models with five and seven substrate segments provide very good approximation of $\boldsymbol{R}_f$. The coupler has been optimized using the ISM surrogate model with five substrate segments (with h fixed to 0.762 mm). The optimized design, obtained in three iterations of the algorithm of Section II, is $\boldsymbol{x}^* = [0.39 \ 5.47 \ 0.21 \ 1.64 \ 0.81]^T$. Responses of the structure at the initial and optimized designs are shown in Fig. 2(b).

The numerical cost of the design optimization process corresponds to about 15 $\boldsymbol{R}_f$ model simulations with the typical cost of PE and SO being about 14 and 25 $\boldsymbol{R}_c$ model evaluations, respectively. For the sake of comparison (see Table I), the coupler was also optimized using conventional SM approaches that exploit equivalent circuit models, i.e., two variants of ISM [7] and a sequential space mapping (SSM) [9].

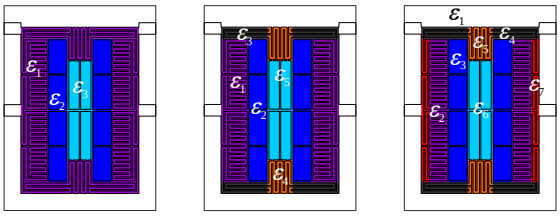

Fig. 1. Conceptual illustration of substrate partitioning for a compact rat-race coupler with varying substrate permittivity ε_k and common substrate height h (not shown) for: (a) three, (b) five, and (c) seven segments.

It should be noted that faster convergence of the EM-based ISM results from better correlation of the EM coarse model compared to equivalent circuit models utilized by benchmark methods. Also, the proposed approach exploits the same solvers for evaluating $\boldsymbol{R}_f$ and $\boldsymbol{R}_c$. This results in simpler implementation compared to conventional SM techniques. Note also, that for the considered RRC, the cost of the EM-based ISM is lower than for ISM and SSM (see Table I), yet this may be due to using a combination of ISM, OSM, and FSM.

The photograph of the manufactured RRC, as well as comparison of its simulated and measured frequency characteristics is shown in Fig. 4. The results are in acceptable agreement. The measured response is slightly shifted down in frequency and features broader –20 dB bandwidth compared to the simulated one. Phase shift, although not considered in the optimization, is also acceptable. Visible discrepancies between characteristics are due to fabrication tolerances and utilization of a simplified EM model that lacks the SMA connector.

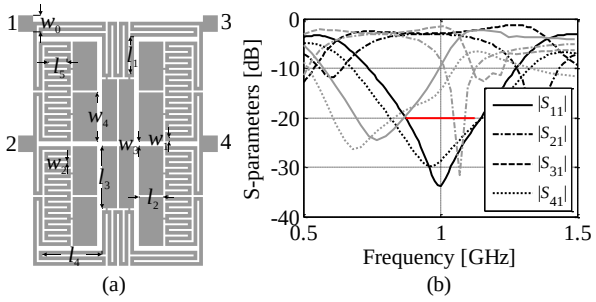

Fig. 2. Considered compact rat-race coupler [1]: (a) geometry and (b) frequency characteristics at the initial (gray) and the optimized design (black) obtained using EM-based ISM with $\boldsymbol{R}_{c2}$.

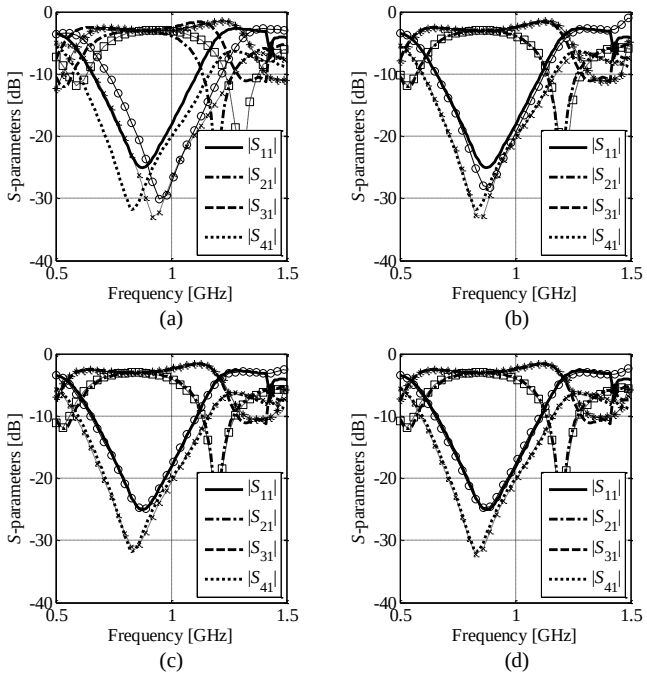

Fig. 3. Fine (thick lines) and coarse (thin lines with markers) models responses at a selected RRC design: (a) $\boldsymbol{R}_c$, (b) $\boldsymbol{R}_{c1}$, (c) $\boldsymbol{R}_{c2}$, (d) $\boldsymbol{R}_{c3}$.

TABLE I
RRC DESIGN: NUMERICAL COST

Method	Number of model evaluations				Design cost	
	SO	PE	Total $\boldsymbol{R}_c$	$\boldsymbol{R}_f$	Total $\boldsymbol{R}_f$	Total [h]
ISM[1#]	–	–	6.3 × $\boldsymbol{R}_f$	10	–	–
ISM[2]	–	–	8.8 × $\boldsymbol{R}_f$	14	22.8	9.1
SSM[2]	–	–	7.3 × $\boldsymbol{R}_f$	11	18.3	7.3
This work	98 × $\boldsymbol{R}_c$	42 × $\boldsymbol{R}_c$	11 × $\boldsymbol{R}_f$	4	15	6

[1] Six parameters – substrate thickness
[2] Twelve parameters – substrate thickness and permittivity
[#] Termination due to divergence

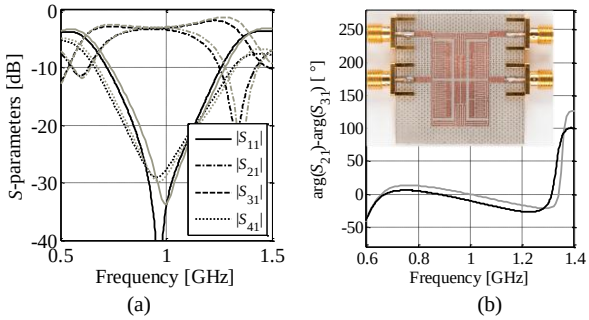

Fig. 4. Comparison of simulated (gray) and measured (black) frequency responses of the RRC: (a) *S*-parameters and (b) phase difference between ports 2 and 3.

IV. CONCLUSION

In this letter, an EM-based implicit space mapping (ISM) for design of complex microwave circuits has been proposed. The method exploits variable-fidelity EM simulations and substrate segmentation. Low-cost surrogate-based optimization and parameter extraction is ensured using trust-region-based framework that keeps derivatives of the structure response unchanged throughout iterations. The method provides better reliability at lower CPU cost compared with conventional SM approaches exploiting an equivalent network coarse models.

REFERENCES

[1] S. Koziel, A. Bekasiewicz, and P. Kurgan, "Rapid design and size reduction of microwave couplers using variable-fidelity EM-driven optimization," *Int. J. RF & Microwave CAE*, vol. 26, no. 1, pp. 27-35, 2016.

[2] J. Kang, S. Rao, P. Chiang and A. Natarajan, "Design and optimization of area-constrained wirelessly powered CMOS UWB SoC for localization applications," *IEEE Trans. Microwave Theory Techn.*, vol. 64, no. 4, pp. 1042-1054, April 2016.

[3] F. Viani, F. Robol, M. Salucci, and R. Azaro, "Automatic EMI filter design through particle swarm optimization" *IEEE Trans. Electrom. Compatibility*, vol. 59, no. 4, pp. 1079-1094, Aug. 2017.

[4] M.A. El Sabbagh, M.H. Bakr, and J.W. Bandler, "Adjoint higher order sensitivities for fast full-wave optimization of microwave filters," *IEEE Trans. Microw Theory Tech.*, vol. 54, pp. 3339-3351, 2006.

[5] S. Koziel and X.S. Yang (Eds.) *Computational Optimization, Methods and Algorithms*, Springer-Verlag, pp. 33-60, 2011.

[6] N.V. Queipo, R.T. Haftka, W. Shyy, T. Goel, R. Vaidynathan, and P.K. Tucker, "Surrogate-based analysis and optimization," *Prog. Aerospace Sci.*, vol. 41, no. 1, pp. 1-28, 2005.

[7] J.W. Bandler, Q.S. Cheng, S.A. Dakroury, A.S. Mohamed, M.H. Bakr, K. Madsen, and J. Søndergaard, "Space mapping: the state of the art," *IEEE Trans. Microwave Theory Tech.*, vol. 52, no. 1, pp. 337-361, 2004.

[8] A. Conn, N.I.M. Gould, P.L. Toint, *Trust-region methods*, MPS-SIAM Series on Optimization, Philadelphia, 2000.

[9] A. Bekasiewicz, P. Kurgan, and M. Kitlinski, "A new approach to a fast and accurate design of microwave circuits with complex topologies," *IET Microwaves, Ant. Prop.*, vol. 6, no. 14, pp. 1616-1622, 2012.